

Osteoarthritis and Cartilage



Brief report

Osteochondral fluid transport in an ex vivo system

Brady David Hislop #, Ara K. Mercer †, Alexandria G. Whitley ‡, Erik P. Myers #, Marie Mackin †, Chelsea M. Heveran #, Ronald K. June # § ¶ *

Department of Mechanical and Industrial Engineering, Montana State University, Bozeman, MT, USA

† Department of Chemistry and Biochemistry, Montana State University, Bozeman, MT, USA

‡ Department of Neuroscience, Johns Hopkins University, Baltimore, MD, USA

§ Department of Cell Biology and Neurosciences, Montana State University, Bozeman, MT, USA

¶ Department of Orthopaedics and Sports Medicine, University of Washington, Seattle, WA, USA

ARTICLE INFO

Article history:

Received 22 October 2023

Accepted 6 February 2024

Keywords:

Bone-to-cartilage fluid transport

Cyclic compression

Mechanotransduction

Osteoarthritis

SUMMARY

Objective: Alterations to bone-to-cartilage fluid transport may contribute to the development of osteoarthritis (OA). Larger biological molecules in bone may transport from bone-to-cartilage (e.g., insulin, 5 kDa). However, many questions remain about fluid transport between these tissues. The objectives of this study were to (1) test for diffusion of 3 kDa molecular tracers from bone-to-cartilage and (2) assess potential differences in bone-to-cartilage fluid transport between different loading conditions.

Design: Osteochondral cores extracted from bovine femurs (N = 10 femurs, 10 cores/femur) were subjected to either no-load (i.e., pure diffusion), pre-load only, or cyclic compression (5 ± 2% or 10 ± 2% strain) in a two-chamber bioreactor. The bone was placed into the bone compartment followed by a 3 kDa dextran tracer, and tracer concentrations in the cartilage compartment were measured every 5 min for 120 min. Tracer concentrations were analyzed for differences in beginning, peak, and equilibrium concentrations, loading effects, and time-to-peak tracer concentration.

Results: Peak tracer concentration in the cartilage compartment was significantly higher compared to the beginning and equilibrium tracer concentrations. Cartilage-compartment tracer concentration and maximum fluorescent intensity were influenced by strain magnitude. No time-to-peak relationship was found between strain magnitudes and cartilage-compartment tracer concentration.

Conclusion: This study shows that bone-to-cartilage fluid transport occurs with 3 kDa dextran molecules. These are larger molecules to move between bone and cartilage than previously reported. Further, these results demonstrate the potential impact of cyclic compression on osteochondral fluid transport. Determining the baseline osteochondral fluid transport in healthy tissues is crucial to elucidating the mechanisms OA pathology.

© 2024 Osteoarthritis Research Society International. Published by Elsevier Ltd. All rights reserved.

Introduction

Osteoarthritis (OA) affects > 500 million people each year.¹ The current standard of care for OA typically includes treatments such as pain management and exercise until an invasive total joint replacement is required. Mechanical and biological interventions that affect the trajectory of OA progression may help mitigate the physical and financial burdens of the disease. However, to design potential

therapeutic interventions, a greater understanding is needed of how fluid is transported between the tissues of the synovial joint.

In the progression of OA, structural and material changes to bone and cartilage may influence fluid transport, with repercussions to the health of the synovial joint.² In OA, the osteochondral interface (cement line to tidemark)³ develops microcracks and is invaded by vasculature, leading to greater fluid transport between bone and uncalcified cartilage.³ Increased fluid transport exposes cartilage to cytokines and proteases produced by bone.^{3,4} These changes occur alongside dysregulation of chondrocyte metabolism, which may contribute to other OA changes (e.g., hypertrophic chondrocytes).^{5,6} The sclerosis of subchondral bone and changes in cartilage permeability may further contribute to differences in how fluid moves within the diseased joint.⁷

* Correspondence to: Mechanical and Industrial Engineering, Montana State University, PO Box 173800, Bozeman, MT 59717-3800, USA.

E-mail address: rjune@montana.edu (R.K. June).

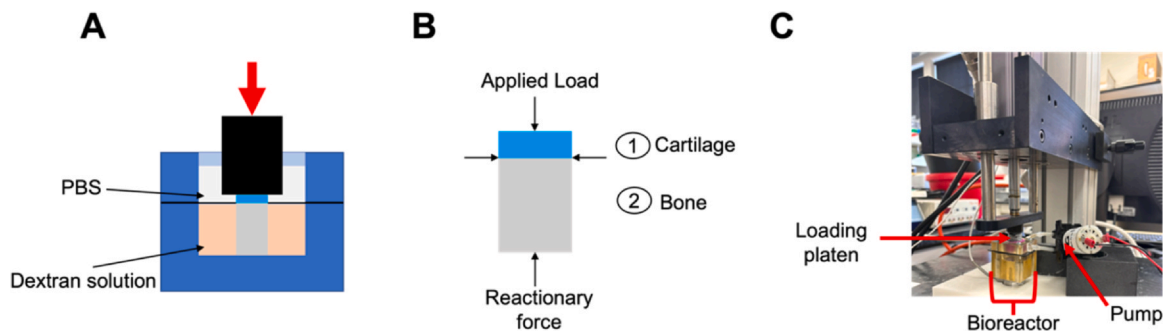


Fig. 1

Osteoarthritis and Cartilage

Schematics and visualization of experimental conditions for osteochondral fluid transport studies A) Cross-section of the bioreactor and loading platen, showing the cartilage fluid chamber with PBS separated from the bone fluid chamber with dextran solution by a rubber sheet. B) Free body diagram showing the forces and boundary conditions acting on the osteochondral cores. C) Experimental set-up for loading studies showing the peristaltic pump attached to the bioreactor circulating the fluid in the cartilage chamber.

While altered fluid transport has been implicated in OA for years,⁷ gaps in understanding persist about how fluid moves between healthy bone and cartilage, and how this transport depends on tissue strain. Fluid transport contributes to mechanosensation and tissue homeostasis in cartilage and bone.^{8,9} In addition, recent data show that small molecules (376 Da, 575 Da, and 1.55 kDa)^{10–12} diffuse from bone-to-cartilage. This is significant because a permeable osteochondral interface suggests new mechanisms for chondrocyte nutrition and cartilage-bone crosstalk (e.g., loading-induced pressure gradients that drive convection). Whether larger molecules can travel from bone-to-cartilage is not yet tested, but is important to understand because biological molecules that would be found within the bone, such as insulin (5 kDa), are at least 3 kDa in size. Furthermore, if the permeability changes with the progression of OA,⁷ the disrupted crosstalk may influence OA progression.³ Deformation-induced interstitial fluid flow may also play an important role in molecular transport from bone-to-cartilage. However, the effects of compression on fluid transport from bone-to-cartilage in healthy tissues are undetermined. Defining the relationship between fluid transport and strain is necessary for improving our understanding of bone-cartilage fluid transport in synovial joints.

In this study, we look to address several critical gaps in our understanding of fluid transport across the osteochondral interface. First, we test for diffusion of 3 kDa fluorescent dextran from bone-to-cartilage. Next, we look to quantify the effect of strain magnitude on bone-to-cartilage fluid transport. Finally, we analyze the effect of strain magnitude on time-to-peak concentration. Measured concentrations for each experimental group were compared to determine the potential effects of strain magnitude and time on bone-to-cartilage fluid transport. The results provide evidence that bone-to-cartilage fluid transport of uncharged molecules at least 3 kDa in size most likely occurs in healthy joints and potentially mediates crosstalk between bone and cartilage through deformation.

Methods

Bovine osteochondral core extraction

Bovine femurs were obtained from a local butcher (N = 20, 10 per experiment). The sample size of n = 10 per experiment was informed by previous fluid tracer studies.¹³ During sample processing, the distal ends of the femurs were hydrated consistently with phosphate-buffered saline (PBS). First, the femur was trimmed to create

two flat surfaces directly posterior to the condyles using a band saw (Supplemental Fig. 1). Next, using an 8 mm bone coring reamer attached to a drill press (Supplemental Fig. 1), ten cores were drilled to a depth of ~20 mm (n = 5 per condyle) and extracted by trimming bone with the band saw. The bone coring tool was continuously hydrated with ice water to minimize temperature increase during coring. After extraction, cores were immediately placed in PBS and stored at -80 °C.

Osteochondral core experimental preparation

Experiments were randomized each experimental day (Supplemental File 1), assigning the cores to an experimental group. Four experimental groups included pure-diffusion (i.e., no-loading), pre-load only, 5 ± 2% cyclical compression (1.1 Hz), or 10 ± 2% cyclic compression (1.1 Hz). On the day of the experiment, cores were removed from the -80 °C freezer and placed in a 37 °C water bath for 5 min. The PBS was then replaced, and the core was allowed to equilibrate for 33 min. After equilibration, cores were trimmed to ~12 mm in height, and the bone face was ground to create a perpendicular angle between the loading platen and the articular surface. A 1/32" thick rubber sheet (McMaster-Carr) with 3 mm diameter centered hole was pulled over the core until snug around the osteochondral interface (Fig. 1A and B), the core was then placed into the bioreactor with the bone side into the bottom chamber (bone fluid chamber).

Experimental procedure

After securing the osteochondral core in the bioreactor (Fig. 1A and B) with the rubber sheet snug around the osteochondral interface, the cartilage chamber was secured to create two separate fluid chambers. 2 mL of 13 μM 3 kDa dextran (Invitrogen)¹³ was then added to the bone chamber through an injection port. The port was then sealed (Gorilla Tough & Clear Double Sided Adhesive Mounting Tape). A peristaltic pump (15 mL/min) was then connected to the fluid ports, and the cartilage chamber was filled with 2 mL of PBS. For all studies, two 100 μL aliquots (t = 0⁻) were immediately sampled from the cartilage chamber and placed in a 96-well plate (Fisherbrand™). For pure-diffusion studies, the sampled fluid was immediately replaced with 200 μL of PBS and the pump was started, after which two more 100 μL aliquots (t = 0⁺) were sampled and again replaced with 200 μL of PBS. Subsequently, aliquots were

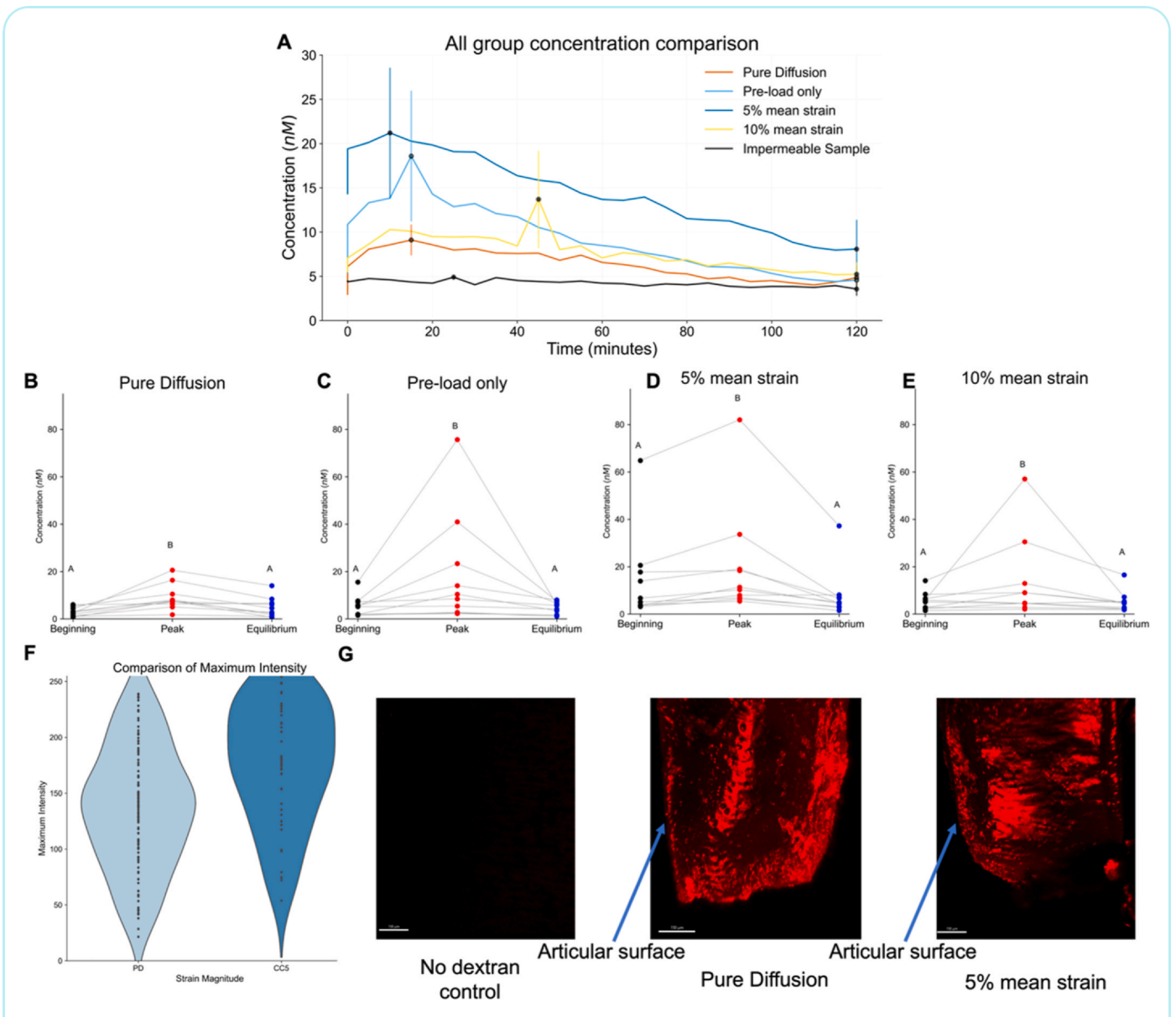


Fig. 2

Comparison of time dynamics of mean tracer concentrations, and line series plots showing changes between beginning (0), peak, and equilibrium (120 min). A) Dynamics of tracer concentration changes over two hours compared to the steady state impermeable tracer concentration. B) Pure-diffusion studies. C) Pre-load only studies. D) 5% mean strain studies. E) 10% mean strain studies. F) Violin plots of maximum fluorescent intensity for pure diffusion v. 5% mean strain. G) Representative confocal images for no dextran control, pure diffusion, and 5% mean strain. For each subplots A-E the letters A and B represent group differences. Data plotted as mean \pm standard error.

sampled with PBS replacement from the cartilage chamber every 5 min for two hours. For pre-load only and cyclical compression studies, a 3.5 N compressive preload was applied (~ 70 kPa), and the position of the loading platen was recorded to define the 0% strain level. Immediately after pre-load two 100 μ L aliquots ($t = 0^+$) were sampled and replaced with 200 μ L of PBS as the cyclic compression experiments were started. Aliquots were then sampled from the cartilage chamber every 5 min for two hours and replaced with 200 μ L of PBS each time. For pre-load only studies, the $t = 0^+$ aliquots were taken ~ 15 s after pre-load. Between each set of aliquots, the 96-well plate was covered with aluminum foil to minimize light exposure. This procedure was repeated with timepoints of 15, 30, 60,

and 120 min before samples were processed for confocal imaging (see [Supplemental Methods](#) and [Supplemental Fig. 2](#)).

Fluorescent intensity studies

Each day, a calibration curve was generated to calculate dextran concentration (1.3 nM–2.8 μ M) from fluorescence intensity. At the end of each experiment the respective plates were analyzed with a fluorescent plate reader (BioTek, Synergy H1 Microplate reader). Excitation/emission of 595/615 nm was used to measure the fluorescent intensity. All concentrations were fit using a 2nd-order polynomial with a zero intercept.

Statistical analysis

Analysis of the dependence of peak intensity on the experimental group

Cartilage fluid chamber concentrations at the beginning ($t=0$), peak, and equilibrium were analyzed using mixed model analysis of variance (ANOVA). The peak tracer concentration was evaluated at 15-minutes for consistency, as the time to peak concentration was not consistent. Fixed effects included strain magnitude (*i.e.*, no-loading, pre-load only, 5% strain, 10% strain), and time-point (*i.e.*, beginning, peak, equilibrium). The random effects in the model included the location on the femur where tissue was harvested and the specimen ID. The model included the interaction term between the fixed effects. Measured concentrations were natural log-transformed, to meet ANOVA assumptions of residual normality and equal variance. *Post hoc* analysis was performed for significant main effects or for interactions while maintaining a family-wise error rate of 0.05 using Tukey's multiple comparisons correction.

Analysis of the dependence of peak intensity on time

The effect of strain magnitude on time-to-peak concentration was analyzed using one-way ANOVA. All assumptions of ANOVA were verified prior to the interpretation of results.

Results

Validation of two-fluid chamber bioreactor

Prior to performing fluorescent tracer concentration studies for the experimental conditions, we validated the baseline change in tracer concentration between the two fluid chambers using an impermeable aluminum cylinder. For all tests ($n=3$), we placed 13 μM dextran solution in the bone fluid chamber. First, we examined the system leakage by placing a rubber sheet with no center hole and found minimal change in tracer concentration in the cartilage chamber. Next, using an aluminum cylinder (8 mm diameter) we determined the baseline tracer concentration increase in the system to be ~ 5 nM (Fig. 2A).

Dextran tracer concentration changes with time and depends on strain

Tracer concentrations in the cartilage fluid chamber were significantly different between time-points ($p < 0.001$), and between strain magnitudes ($p = 0.011$) (Fig. 2, Supplemental Table 1). *Post hoc* comparisons of time points revealed a significantly higher tracer concentration at peak compared to both beginning ($p < 0.001$, (1.499, 2.95) nM) and equilibrium ($p < 0.001$, (1.617, 3.187) nM) times, demonstrating osteochondral fluid transport from bone-to-cartilage. Furthermore, *post hoc* comparisons of strain magnitudes revealed significantly higher tracer concentrations for the 5% mean strain magnitude compared to the pure-diffusion group ($p < 0.005$, (-1.013, -1.136) nM). All other *post hoc* comparisons were not significant. These results suggest that 5% mean strain impacts the transport of 3 kDa dextran molecules from bone-to-cartilage.

Comparison of time to peak equilibrium reveals no effect of experimental condition

The time-to-peak tracer concentration was not significantly impacted by experimental conditions ($p = 0.450$).

Image maximum intensity changes with position, strain magnitude, and time-point

Imaging data show that there is fluorescent signal found throughout the cartilage samples at 15 min after immersion in the

2-chamber bioreactor (Fig. 2, Supplemental Fig. 2, Supplemental Imaging Figures). Maximum intensities of fluorescently labeled fluid within articular cartilage were significantly different between imaging location ($p = 0.004$), strain magnitude ($p = 0.001$), and time-point ($p = 0.001$). *Post hoc* comparisons of strain magnitudes revealed significantly higher maximum fluorescent intensities in the 5% mean strain group compared to the pure diffusion group ($p = 0.006$) and the 10% mean strain group compared to the pure diffusion group ($p = 0.026$), no difference was found between 5% and 10% mean strain. *Post hoc* comparisons of time points revealed significantly higher maximum fluorescent intensities in 120 min when compared to both 30 min ($p = 0.014$) and 60 min ($p = 0.001$), whereas no differences were found between any other time points. Furthermore, *post hoc* comparisons of imaging locations revealed significantly higher fluorescent concentrations at the radial edges ($p = 0.004$).

Discussion

Osteochondral fluid transport has long been neglected in the literature until the onset of OA where vascular invasion into articular cartilage is observed.³ The osteochondral interface has been considered to be an impermeable boundary preventing molecular crosstalk between bone and cartilage.³ Thus, synovial fluid is often considered the sole source of articular cartilage nutrition. However, recent studies with small tracer molecules and the data presented here show the limitations of this prior understanding.^{11,14}

This study provides novel data on the transport of 3 kDa molecules from bone-to-cartilage (*i.e.*, osteochondral fluid transport) in an *ex vivo* osteochondral core system. We found that tracer concentrations changed with time, reaching a peak a few minutes after the start of the experiment. These results, together with prior studies with smaller molecules (*e.g.*, 376 Da), provide evidence that uncharged molecules can move from bone-to-cartilage.¹¹ Bone is highly metabolically active and small molecules produced by this tissue could have roles in crosstalk with cartilage that are currently underappreciated. Future studies should consider molecule size, charge, and shape on diffusion from bone-to-cartilage.¹⁵

We also investigated whether fluid transport between bone and cartilage depends on the magnitude of cyclic compressive strain. Our results demonstrate that the $5\% \pm 2\%$ strain increases the peak tracer concentration compared with the pure-diffusion condition. Furthermore, results from our imaging studies also demonstrated that $5\% \pm 2\%$ strain increases fluorescent intensity when compared to pure-diffusion studies. Interestingly, the other strain groups did not differ from pure-diffusion. A potential explanation for this lack of influence by the larger strain could be that the cartilage was not fully unloaded (*i.e.*, tissues were unloaded to 8% strain). It is possible that pore networks of cartilage cannot fully open without greater unloading, limiting the ability of fluid to convectively and/or diffusively move from bone-to-cartilage. The range of 3%–7% cyclic strain in the lower strain magnitude group may better allow the opening and closing of pore networks in cartilage. However, whether pore network opening in cartilage is an important regulator of convective fluid transport from bone-to-cartilage requires further investigation. Studies should consider a greater range of peak and unloading strains as well as strain rates.

Finally, we investigated the impacts of strain magnitude on time-to-peak concentration. Time-to-peak concentration was not significantly impacted by strain magnitude. These results support our findings of convective fluid transport from bone-to-cartilage, as time-to-peak is not affected by strain magnitude, suggesting that strain is not significantly impacting bone-to-cartilage diffusion.

There are several limitations to this study. Sampling every five minutes and replacing in volume limited our temporal resolution

and likely diluted cartilage fluid chamber concentration. Future studies should consider building a fluorescent measurement system capable of higher sampling frequency. Future studies should couple tracer concentration and imaging to visualize the movement of a tracer into cartilage. A final limitation is that the studies using an impermeable surrogate found a small amount of leakage around the seal, indicating that a small amount of the observed cartilage-side fluorescence may have resulted from leakage. Finally, our study does not consider tissue mechanical properties and their impact on bone-to-cartilage fluid transport. Future studies should incorporate finite element modeling to study the correlation between bone-to-cartilage molecular flux and tissue mechanical properties.

In conclusion, we found bone-to-cartilage fluid transport in an *ex vivo* system, suggesting that the current paradigm of an impermeable osteochondral interface should be reconsidered. The implications of increased bone-to-cartilage fluid transport in health are not well understood and need significant future investigation. By establishing the baseline molecular flux from bone-to-cartilage we will improve our understanding of joint physiology, which may lead us one step closer to new treatments for OA.

Author contributions

Experimental design: BDH, RKJ; Bioreactor Development: BDH, EPM, RKJ; Data collection: BDH, AKM, AGW; Data analysis and interpretation: BDH, CMH, RKJ; Manuscript drafting: BDH, RKJ; Revision of manuscript: all authors; Approval of manuscript: all authors.

Role of the funding source

This work was supported by grants from the National Institutes of Health (NIAMS R01AR073964 and R01AR081489) and the National Science Foundation (CMMI 1554708). This work represents the views of the authors and not necessarily those of the sponsors.

Conflict of Interest

Dr. June owns stock in Beartooth Biotech and OpenBioWorks, which were not involved in this study.

Acknowledgments

We would like to thank Dr. Priyanka Brahmachary for procuring the bovine femurs, and Alexander Springer for helping with the initial experimentation.

Appendix A. Supporting information

Supplementary data associated with this article can be found in the online version at [doi:10.1016/j.joca.2024.02.946](https://doi.org/10.1016/j.joca.2024.02.946).

References

1. Long H, Liu Q, Yin H, Wang K, Diao N, Zhang Y, et al. Prevalence trends of site-specific osteoarthritis from 1990 to 2019: Findings from the Global Burden of Disease Study 2019. *Arthritis Rheumatol* 2022;74:1172–83.
2. Carlson AK, Rawle RA, Adams E, Greenwood MC, Bothner B, June RK. Application of global metabolomic profiling of synovial fluid for osteoarthritis biomarkers. *Biochem Biophys Res Commun* 2018;499:182–8.
3. Yuan XL, Meng HY, Wang YC, Peng J, Guo QY, Wang AY, Lu SB. Bone-cartilage interface crosstalk in osteoarthritis: potential pathways and future therapeutic strategies. *Osteoarthr Cartil* 2014;22:1077–89.
4. Westacott CI, Webb GR, Warnock MG, Sims JV, Elson CJ. Alteration of cartilage metabolism by cells from osteoarthritic bone. *Arthritis Rheum* 1997;40:1282–91.
5. Martin JA, Buckwalter JA. Aging, articular cartilage chondrocyte senescence and osteoarthritis. *Biogerontology* 2002;3:257–64.
6. Zheng L, Zhang Z, Sheng P, Mobasher A. The role of metabolism in chondrocyte dysfunction and the progression of osteoarthritis. *Ageing Res Rev* 2021;66, 101249.
7. Hwang J, Bae WC, Shieu W, Lewis CW, Bugbee WD, Sah RL. Increased hydraulic conductance of human articular cartilage and subchondral bone plate with progression of osteoarthritis. *Arthritis Rheum* 2008;58:3831–42.
8. Sah RL, Kim YJ, Doong JY, Grodzinsky AJ, Plaas AH, Sandy JD. Biosynthetic response of cartilage explants to dynamic compression. *J Orthop Res* 1989;7:619–36.
9. Fritton SP, Weinbaum S. Fluid and solute transport in bone: flow-induced mechanotransduction. *Annu Rev Fluid Mech* 2009;41:347–74.
10. Burstein D, Velyvis J, Scott KT, Stock KW, Kim YJ, Jaramillo D, et al. Protocol issues for delayed Gd(DTPA)(2-)-enhanced MRI (dGEMRIC) for clinical evaluation of articular cartilage. *Magn Reson Med* 2001;45:36–41.
11. Pan J, Zhou X, Li W, Novotny JE, Doty SB, Wang L. In situ measurement of transport between subchondral bone and articular cartilage. *J Orthop Res* 2009;27:1347–52.
12. Pouran B, Arbabi V, Bleys RL, Rene van Weeren P, Zadpoor AA, Weinans H. Solute transport at the interface of cartilage and subchondral bone plate: Effect of micro-architecture. *J Biomech* 2017;52:148–54.
13. Leddy HA, Guilak F. Site-specific molecular diffusion in articular cartilage measured using fluorescence recovery after photobleaching. *Ann Biomed Eng* 2003;31:753–60.
14. Pan J, Wang B, Li W, Zhou X, Scherr T, Yang Y, et al. Elevated cross-talk between subchondral bone and cartilage in osteoarthritic joints. *Bone* 2012;51:212–7.
15. Pluen A, Netti PA, Jain RK, Berk DA. Diffusion of macromolecules in agarose gels: comparison of linear and globular configurations. *Biophys J* 1999;77:542–52.